

# The Effects of the NaF Flux on the Oxidation State and Localisation of Praseodymium in Pr-doped Zircon Pigments

Manuel Ocaña,<sup>a\*</sup> Alfonso Caballero,<sup>a</sup> Agustín R. González-Elipe,<sup>a</sup> Pedro Tartaj,<sup>b</sup> Carlos J. Serna<sup>b</sup> and Rosa I. Merino<sup>c</sup>

<sup>a</sup>Instituto de Ciencia de Materiales de Sevilla, C.S.I.C.-Universidad de Sevilla, Americo Vespucio s/n, Isla de La Cartuja, 41092 Sevilla, Spain

<sup>b</sup>Instituto de Ciencia de Materiales de Madrid, C.S.I.C., Campus Universitario de Cantoblanco, 28049 Cantoblanco, Madrid, Spain

<sup>c</sup>Instituto de Ciencia de Materiales de Aragón, C.S.I.C.-Universidad de Zaragoza, Facultad de Físicas, Plaza San Francisco s/n, 50009 Zaragoza, Spain

(Received 10 July 1998; accepted 30 August 1998)

## Abstract

*The role that NaF plays in the preparation of Pr-doped zircon pigments was studied through the analysis of the nature and localisation of the Pr cations into the zircon matrix in samples prepared in the absence and in the presence of NaF. As previously observed, the addition of NaF caused a decrease of the minimum temperature required for zircon formation from 1400 to 1100°C, and an increase of the yellow colour intensity. In the absence of NaF, the Pr cations mainly presented a threefold oxidation state, being located out of the zircon lattice as Pr<sub>2</sub>Zr<sub>2</sub>O<sub>7</sub>, whereas in the presence of this flux, most of the Pr cations showed a fourfold valence and formed a solid solution with the zircon lattice, which was then the main responsible for the stronger yellow colour observed in this case. After heating this pigment at 1400°C, we detected an exsolution of the Pr (IV) cations as Pr<sub>8</sub>Si<sub>6</sub>O<sub>24</sub> which was accompanied by a decrease of the yellow colour intensity. Therefore, it was concluded that the main role of NaF in the preparation of yellow Pr-zircon pigments is to decrease the temperature of zircon formation to the range in which the chromophore responsible for the bright yellow colour, i.e. the Pr (IV)-zircon solid solution, is stable. © 1999 Elsevier Science Limited. All rights reserved*

**Keywords:** colour, zircon, defects, spectroscopy, optical properties.

## 1 Introduction

The need for clean and bright yellow colours in the ceramic pigments field led to the development of praseodymium-doped zircon (Pr–ZrSiO<sub>4</sub>) in the late 1950s.<sup>1</sup> The yellow colour of this pigment is developed when an equimolecular mixture of SiO<sub>2</sub> and ZrO<sub>2</sub> containing a source of praseodymium (usually Pr<sub>6</sub>O<sub>11</sub>) is calcined up to zircon formation.<sup>2</sup> The commercial production of Pr–ZrSiO<sub>4</sub> also includes the addition of a certain amount of fluxes (normally NaF) to the starting oxides mixture since it was observed that a much stronger and brighter colour resulted under these conditions.<sup>1–3</sup> As expected, such an addition also produced a decrease of the temperature required for zircon crystallization.<sup>4,5</sup>

In spite of the technological importance of Pr–ZrSiO<sub>4</sub>, only a few papers have dealt with the role that NaF play in the formation of this pigment.<sup>6–8</sup> In general, these works have been focused on kinetic aspects concluding that the acceleration of zircon crystallisation produced by NaF takes place through the formation of SiF<sub>4</sub> which volatilises thus favouring the transport of Si<sup>4+</sup> ions to the zirconia phase.<sup>6</sup> However, up to our knowledge, no experimental data have been reported to justify the differences in colour properties detected between samples prepared in the absence or the presence of NaF.

The aim of this work is to study the effects of the addition of NaF on the nature and localisation of the Pr species in the zircon matrix of Pr-doped zircon powders and therefore, on their colour properties.

\*To whom correspondence should be addressed

For such a purpose, the Pr–ZrSiO<sub>4</sub> samples were prepared by the hydrolysis of liquid aerosols, which as it has been recently reported for other zircon pigments, may produce stronger colours than the traditional ceramic or sol–gel methods.<sup>9</sup> The thermal evolution of these Pr–ZrSiO<sub>4</sub> powders as prepared and after the addition of NaF, was studied in detail in order to optimise the colour properties of the resulting pigments.

## 2 Experimental

### 2.1 Samples preparation

The preparation of the praseodymium-doped zircon powders was carried out by hydrolysis of liquid aerosols, using a procedure similar to that previously reported to obtain several ceramic pigments.<sup>9–12</sup> Essentially, it involves the generation and further hydrolysis of a liquid aerosol consisting of an equimolecular mixture of silicon ethoxide (TEOS, Fluka, 98%) and zirconium propoxide (Aldrich, technical grade) to which an aliquot of a solution of PrCl<sub>3</sub>·6H<sub>2</sub>O (Aldrich, 99.9%) in ethanol was added before aerosol generation. Owing to the much lower hydrolysis rate of TEOS when compared to zirconium propoxide, in order to obtain the zircon stoichiometry (Zr/Si = 1), the mixture of the two alkoxides was partially hydrolysed for 24 h at 20°C in an atmosphere of 60% relative humidity<sup>13</sup> before the addition of the praseodymium salt. The final liquid mixture was nebulised and hydrolysed at room temperature as previously described,<sup>9</sup> and the resulting powders were collected by using nylon sieves. The Pr/Zr mole ratio selected for this work was 0.09 (Table 1) since the use of higher values is not expected to produce stronger colour.<sup>1</sup>

The Pr–ZrSiO<sub>4</sub> samples as prepared or after the addition of NaF (NaF/ZrSiO<sub>4</sub> mole ratio = 0.2) were heated for 8 h at the desired temperatures in platinum crucibles at a heating rate of 10°C min<sup>-1</sup>.

### 2.2 Characterisation

The particle size and shape of the powders were examined by scanning (SEM, JEOL JSM5400)

**Table 1.** Composition (Si/Zr and Pr/Zr atomic ratios) measured by ICP for the Pr-doped zircon sample as prepared and after heating at different temperatures in the presence or the absence of NaF. The Pr/Zr ratio obtained from the XPS spectra of the heated samples is also included

Sample	(Si/Zr) (atomic)	(Pr/Zr) (atomic) ICP	(Pr/Zr) (atomic) XPS
As prepared	0.94	0.091	—
Heated at 1400°C	0.96	0.092	3.8
Heated at 1100°C/NaF	0.82	0.075	20.5

electron microscopy.

The composition of the solids (Zr/Si ratio and Pr content) was determined by plasma emission (ICP, Perkin Elmer, Model 5500). For this purpose, 100 mg of sample were first fused at 1100°C with a NaKCO<sub>3</sub>:Na<sub>2</sub>B<sub>4</sub>O<sub>7</sub> mixture and then extracted with a HCl solution. The presence or absence of chlorine in the samples was assessed by EDX (Link ISIS).

The different phases present in the solids were identified by X-ray diffraction (Siemens D501). The unit cell parameters of the powders were measured by Rietveld analysis of the X-ray diffraction data following the procedure described in Ref. 14. In all experiments a silicon standard (20% by weight) was mechanically mixed with the pigment. The crystallographic data for zircon and silicon were taken from Ref. 15 and 16, respectively.

Differential thermal (DTA) and thermogravimetric (TGA) analyses (Setaram 92-16-18) were carried out in air at a heating rate of 10°C min<sup>-1</sup>.

The electron paramagnetic resonance (EPR) measurements were performed in a Bruker ESP-300E spectrometer, in the X-band. The samples were cooled in a flowing helium cryostat and the measurements performed between 4.2 and 10 K. The microwave frequency was measured with a HP-5350B frequency counter. XPS spectra were obtained with a VG Escalab 220 model using the MgK<sub>α</sub> excitation source. Calibration of the spectra was done at the C1s peak of surface contamination taken at 284.6 eV. Atomic percentages of the elements were calculated from the peaks areas after background subtraction (Shirley background). The areas were referred to the sensitivity factors of the elements as supplied by the instrument manufacturers.

In order to analyse the XANES spectra, Pr (III) acetate and Pr<sub>6</sub>O<sub>11</sub> were used as reference compounds for the trivalent and tetravalent state of Pr, respectively. Notice that in the latter, two different oxidation states of Pr (3+ and 4+) are actually present, although it contains a higher amount (~67%) of Pr<sup>4+</sup>. XANES spectra were collected at the LURE synchrotron facility in Orsay, using synchrotron radiation from the DCI storage ring running at 1.85 GeV with an average current of 250 mA. The XANES data were taken at room temperature in the transmission mode using two ion chambers containing a He–Ne mixture as detectors. Monochromatization of the light was done with a double-crystal monochromator [Si(111)]. For measurements, the Pr-doped zircon sample and the references, Pr (III) acetate and Pr<sub>6</sub>O<sub>11</sub>, were dispersed in boron nitride in order to optimise the absorptions. Three-four scans were collected for each sample and averaged. The spectra were analysed with the software package

developed by Bonin *et al.*<sup>17</sup>

The colour of the pigments was determined according to the Commission Internationale de l'Éclairage (CIE) through  $L^*a^*b^*$  parameters.<sup>18</sup> In this system,  $L^*$  is the colour lightness ( $L^*=0$  for black and  $L^*=100$  for white),  $a^*$  is the green (–)–red (+) axis, and  $b^*$  is the blue (–)–yellow (+) axis. These parameters were measured for an illuminant D 65, using a Dr Lange, LUCI 100 colorimeter and a white tile ceramic having chromaticity coordinates ( $x=0.315$ ,  $y=0.335$ ) as standard reference. For measurements, 40 mg of pigment were dispersed in doubly distilled water and filtered through  $0.22\ \mu\text{m}$  Millipore filters, resulting in a thin layer with a density of  $6\ \text{mg cm}^{-1}$ . This amount was sufficient to avoid substrate effects on colour measurements.

### 3 Results and Discussion

#### 3.1 Preparation of pigments

The as prepared Pr-ZrSiO<sub>4</sub> powders consisted of spherical ( $0.1\text{--}5\ \mu\text{m}$ ) particles [Fig. 1(A)] which were amorphous to X-ray diffraction. The DTA curve obtained for this sample (Fig. 2) showed an endothermic effect centred at  $125^\circ\text{C}$  accompanied by a weight loss of 24% (between  $25$  and  $400^\circ\text{C}$ ) as detected by TGA (Fig. 1), which is due to the desorption of water and adsorbed alcohols produced as by-products of the alkoxides hydrolysis.<sup>13</sup> Two exothermic peaks were also observed at  $780$  and  $880^\circ\text{C}$ , respectively. The first one can be attributed to the crystallisation of metastable tetragonal zirconia (t-ZrO<sub>2</sub>) as indicated by the X-ray diffraction pattern of the sample heated at  $800^\circ\text{C}$  (Fig. 3). It should be noted that this process takes place at lower temperature in this sample than in undoped zircon powders prepared by a similar procedure.<sup>13</sup> As it has been suggested for Fe-doped zircon,<sup>14</sup> such a kinetic effect could be explained by the formation of a solid solution between the Pr cations and the zirconia lattice, as expected from the behaviour previously reported for some other rare earth,<sup>19</sup> and indicated by a shift of the X-ray diffraction peaks of the heated sample to lower  $d$ -spacing values respect to those corresponding to undoped tetragonal zirconia.<sup>20</sup> The last exothermic effect at  $880^\circ\text{C}$  can be ascribed to the release of chlorine coming from the Pr salt, as confirmed by EDX analyses of the sample. The weight loss of 2.2% detected by TGA at the same temperature is in agreement with this interpretation. No additional effects were detected by thermal analysis up to  $1500^\circ\text{C}$ , however, X-ray diffraction (Fig. 3) revealed some other structural changes in the sample on calcination at  $>1100^\circ\text{C}$ . Thus, the onset of

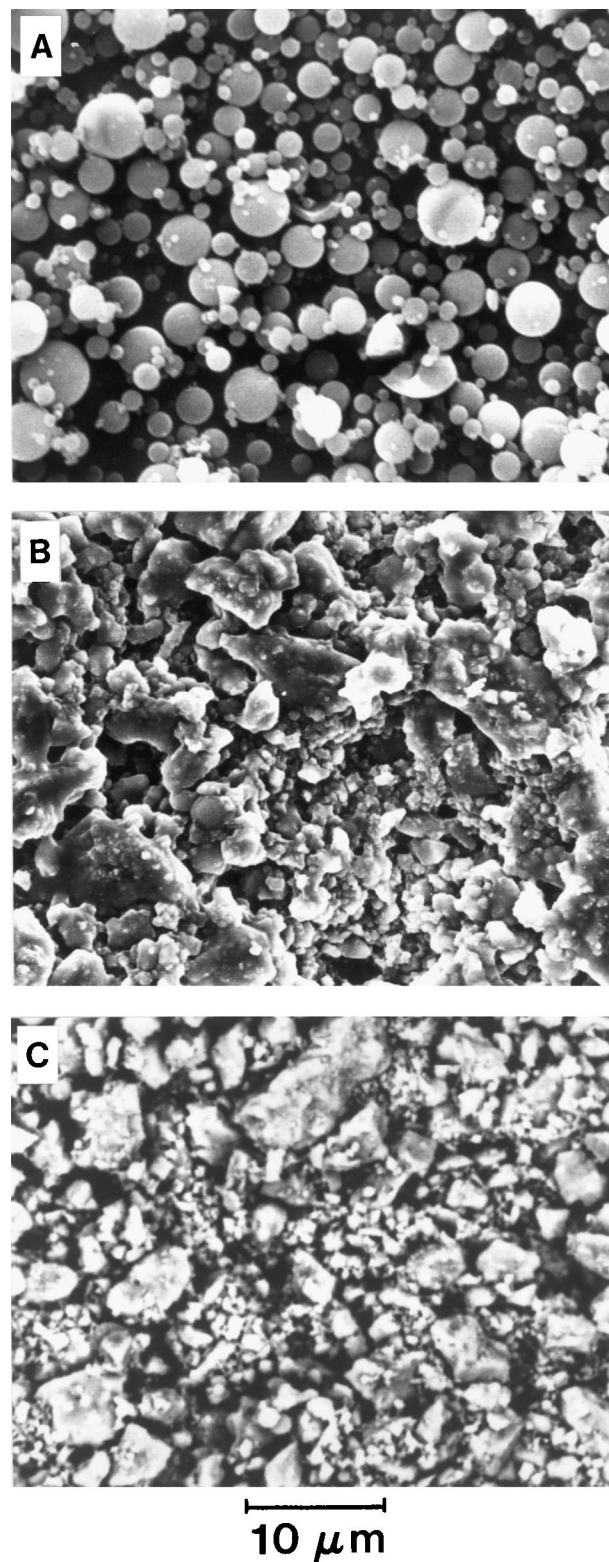


**Fig. 1.** Scanning electron micrographs of the Pr-doped zircon powders as prepared (A) and after heating at  $1400^\circ\text{C}$  in the absence of NaF (B) and at  $1100^\circ\text{C}$  in the presence of NaF (C).

zircon formation was detected at  $1200^\circ\text{C}$ , being accompanied by a partial phase transformation from tetragonal to monoclinic (m-ZrO<sub>2</sub>) zirconia, which must be produced during the cooling process.<sup>21</sup> The fraction of crystallised zircon increased at increasing temperature being maximum at  $1400^\circ\text{C}$ . At this temperature, some weak peaks

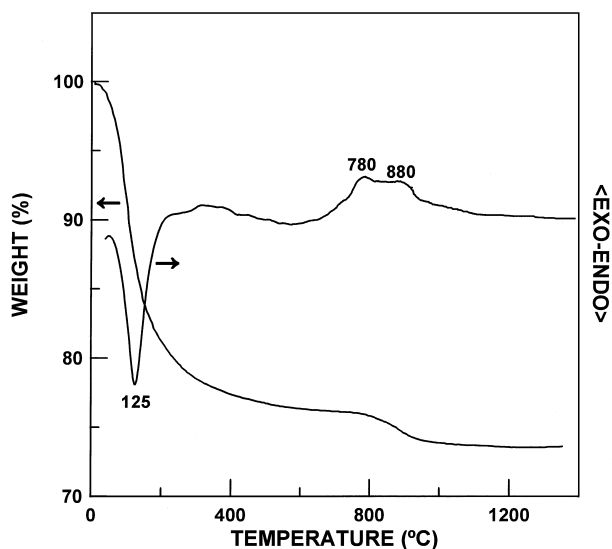


Fig. 2. Differential thermal and thermogravimetric curves obtained for the Pr-doped zircon sample.

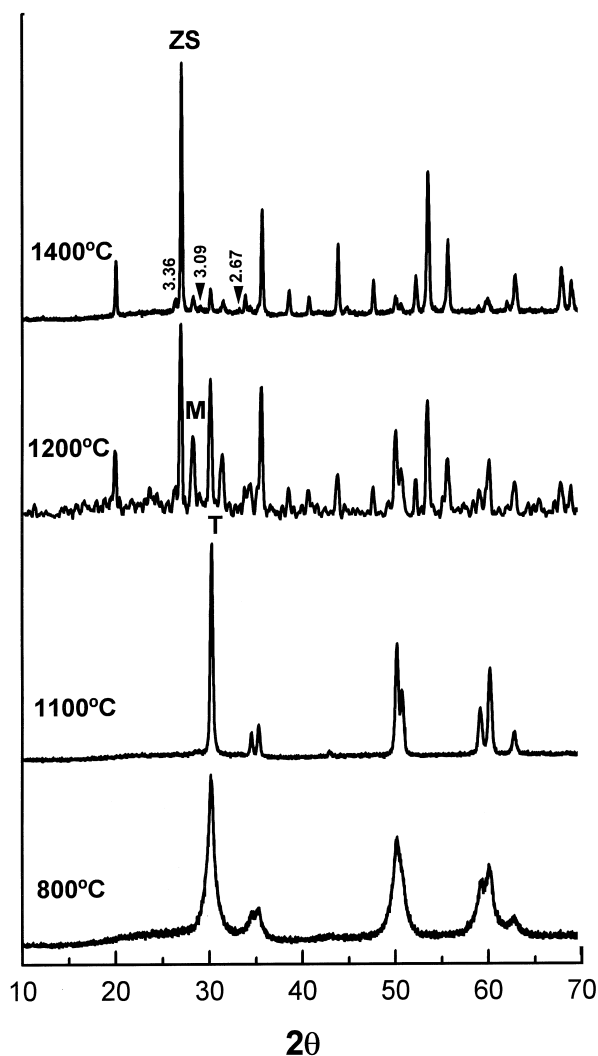


Fig. 3. X-ray diffraction patterns of the Pr-doped zircon sample heated at different temperatures in the absence of NaF. Symbol designating the most intense reflections of the different phases: ZS=zircon, M=monoclinic zirconia and T=tetragonal zirconia.

corresponding to unreacted t-ZrO<sub>2</sub> and m-ZrO<sub>2</sub> still remained in the pattern as expected from the little excess of Zr (Si/Zr=0.94) present in the sample (Table 1). Several additional weak peaks were also detected at *d*-spacing values of 3.36, 3.09 2.67 Å (Fig. 3), which can be more clearly observed in the magnified pattern shown in Fig. 4. Whereas the two latter peaks could be associated to some of the most intense reflections of Pr<sub>2</sub>Zr<sub>2</sub>O<sub>7</sub><sup>22</sup> the first one (*d*=3.36Å) could not be assigned to any known Pr compound. No further changes were observed by X-ray diffraction in the sample heated up to 1500°C. It should be noted that after zircon formation ( $\geq 1400^\circ\text{C}$ ) the particles sintered losing their spherical shape [Fig. 1(b)].

The  $L^*a^*b^*$  parameters of the sample heated at 1400°C ( $L^*=82$ ,  $a^*=-3.5$  and  $b^*=20$  corresponded to a weak yellow colour and remained unchanged after heating at 1500° (Table 2).

As shown by X-ray diffraction (Fig. 5) the addition of NaF to the starting amorphous Pr-ZrSiO<sub>4</sub> powders considerably lowered the minimum temperature required for zircon formation (1100°C) respect to the corresponding one in the absence of this flux (1400°C), in agreement with the kinetic effect of the latter previously reported.<sup>4-7</sup> However, the amount of unreacted zirconia detected after this treatment increased (Fig. 3 and Fig. 5), which could be associated to the decrease detected

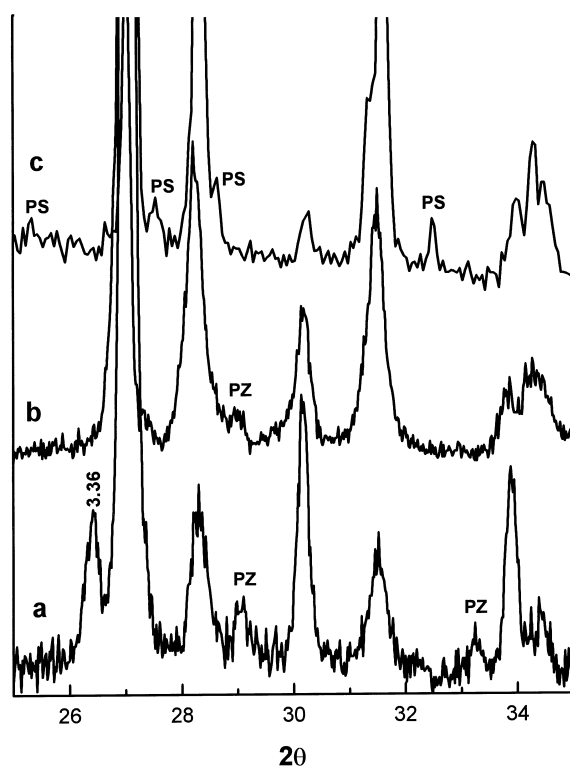
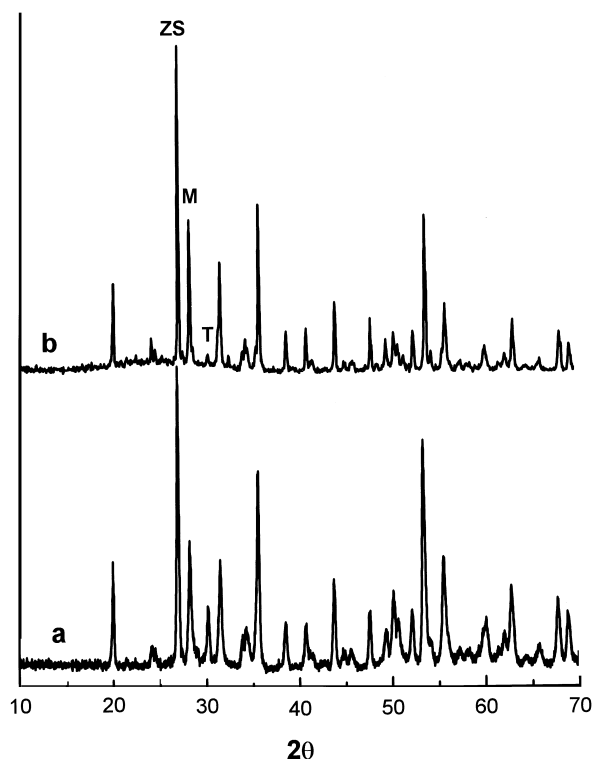


Fig. 4. Magnified X-ray diffraction patterns of the Pr-doped zircon sample heated at: (a) 1400°C in the absence of NaF, (b) 1100°C in the presence of NaF and (c) the same as in (b) followed by an additional heating at 1400°C. The peaks ascribed to Pr<sub>2</sub>Zr<sub>2</sub>O<sub>7</sub> (PZ) and Pr<sub>4</sub>Si<sub>6</sub>O<sub>24</sub> (PS) have been marked.



**Fig. 5.** X-ray diffraction patterns of the Pr-doped zircon sample heated at different temperatures in the presence of NaF: (a) 1100°C and (b) the same as in (a) followed by an additional heating at 1400°C. Symbols designating the most intense reflections of the different phases: ZS = zircon, H = monoclinic zirconia, T = tetragonal zirconia.

for the Si/Sr ratio (0.82) (Table 1), probably due to a partial volatilisation of Si. This observation is also in favour of the mechanism previously proposed for zircon crystallisation in the presence of NaF, according to which a volatile Si compound ( $\text{SiF}_4$ ) is formed as an intermediate step.<sup>6</sup> It should be noted that under these conditions the amount of Pr contained in the sample slightly decreased ( $\text{Pr}/\text{Zr} = 0.076$ ) (Table 1) upon calcination. This behaviour, which was not observed in the absence of NaF (Table 1), seems to indicate the formation of a certain volatile Pr compound during calcination as previously suggested.<sup>7,8</sup> Finally, the weak reflection with  $d$  spacing at 3.36 Å and most of the additional peaks corresponding to  $\text{Pr}_2\text{Zr}_2\text{O}_7$  could not be detected in the X-ray diffraction pattern of the sample heated at 1100°C in the presence of NaF, except the one at  $d = 3.09$  Å, which showed lower intensity than in the absence of the flux (Fig. 4). As expected, the addition of the flux agent resulted in

**Table 2.**  $L^*a^*b^*$  parameters of the Pr-doped zircon sample heated at different temperatures in the absence or the presence of NaF

Temperature	$L^*$	$a^*$	$b^*$
1400°C	82.0	-3.5	20
1500°C	82.1	-3.4	20
1100°C/NaF	80.0	-1.0	54
1100°C/NaF + 1400°C	83.0	-3.5	35

the formation of irregular particles after calcination [Fig. 1(C)].

In agreement with previous observations, the yellow colour of the sample heated at 1100°C after the addition of NaF was stronger and brighter than that resulting in the absence of the flux, as clearly manifested by the much higher value of  $b^*$  (54) showed by the former (Table 2). To explain such colour differences, the oxidation state and the localisation of the Pr cations in the pigments NaF were investigated.

### 3.2 Origin of colours

The ESR spectra of the Pr-doped zircon powders heated in the absence and the presence of NaF were measured to analyse the oxidation state of the Pr species in both samples. The spectra taken at 10 K with minimum microwave power (Fig. 6) displayed in both cases six main lines, which are due to  $\text{Pr}^{4+}$  ( $I = 5/2$ ), as revealed by the good agreement with the line positions calculated using the parameters reported for  $\text{Pr}^{4+}$  in a  $\text{ZrSiO}_4$  single crystal ( $g_{\parallel} = 1.0038$ ,  $g_{\perp} = 1.0384$ ,  $A_{\parallel} = 0.06045 \text{ cm}^{-1}$  and  $A_{\perp} = 0.06386 \text{ cm}^{-1}$ ).<sup>23</sup> Although the spectrum of the sample heated in the absence of NaF showed some degree of saturation, a comparative estimation of the amount of  $\text{Pr}^{4+}$  in both samples could be made. Thus, it was found that the amount of this cation in the sample heated in the absence of NaF was much lower (between 10 and 20%) than that contained in the sample heated in the presence of this flux. This suggests the presence in the former sample of an important amount of Pr with a different oxidation state, since the total Pr content in both samples was similar (Table 1). In agreement, the  $\text{Pr}_2\text{Zr}_2\text{O}_7$  phase detected by X-ray diffraction in the sample heated in the absence of the flux (Figs 3 and 4) indicates the presence of  $\text{Pr}^{3+}$  which is a non-Kramers ion and it was not detected by ESR.

It must be noted that the broadening of the ESR lines in our samples was much higher than that previously reported for Pr- $\text{ZrSiO}_4$  single crystals.<sup>23</sup> This finding suggests a strong dipolar interaction between paramagnetic centres ( $\text{Pr}^{4+}$ ) in the pigments probably as a consequence of agglomeration of the Pr cations within the zircon matrix. This suggestion agrees with the Pr/Zr mole ratio obtained from the XPS spectra of the samples, which was much higher than that corresponding to the bulk material (Table 1) indicating an important enrichment of Pr in the particle outer layers.

In order to gain additional information on the nature of the Pr species incorporated into the Pr-doped zircon powders, we also analysed their  $L_{III}$  edge XANES spectrum (Fig. 7), which, as previously shown,<sup>24,25</sup> can be qualitatively used as a fingerprint of the oxidation state of Pr cations.

Thus, as observed in the spectrum of the Pr (III) acetate reference (Fig. 7), the  $\text{Pr}^{3+}$  valence is characterised by a single white line maximum at 5954 eV (A) due to the  $2p \rightarrow 6d$  transition in  $\text{Pr}^{3+}$ .<sup>24</sup> On the other hand, the spectrum of  $\text{Pr}^{4+}$  displays two white lines at 5954 and 5965 eV as a result of the configuration interaction due to a large mixing between localised 4f levels of Pr and more delocalised O 2p levels.<sup>24,25</sup> Such features (B and C) can be observed in the spectrum of  $\text{Pr}_6\text{O}_{11}$  also included in Fig. 7 as a reference. Notice that in this oxide,  $\sim 33\%$  of the total Pr content corresponds to  $\text{Pr}^{3+}$ . Therefore, the line at 5954 eV has contribution from the  $\text{Pr}^{4+}$  ions as well as from the  $\text{Pr}^{3+}$  ions, whereas the line at 5965 eV is only due to  $\text{Pr}^{4+}$ .

In our case, the spectrum of the sample heated in the absence of NaF is similar to that of Pr (III) acetate, indicating that most of the Pr cations in this sample are in a trivalent state, which would be in agreement with the low amount of  $\text{Pr}^{4+}$  detected by ESR (Fig. 6) and the presence of  $\text{Pr}_2\text{Zr}_2\text{O}_7$  suggested by X-ray diffraction (Figs 3 and 4). However, the spectrum of the sample heated in the presence of NaF showed two white lines as  $\text{Pr}_6\text{O}_{11}$ , manifesting the presence of  $\text{Pr}^{4+}$ . It should be noted that although the intensity of the two white lines of  $\text{Pr}^{4+}$  also depend on the metal–ligand bonding, the lower relative intensity of the line at

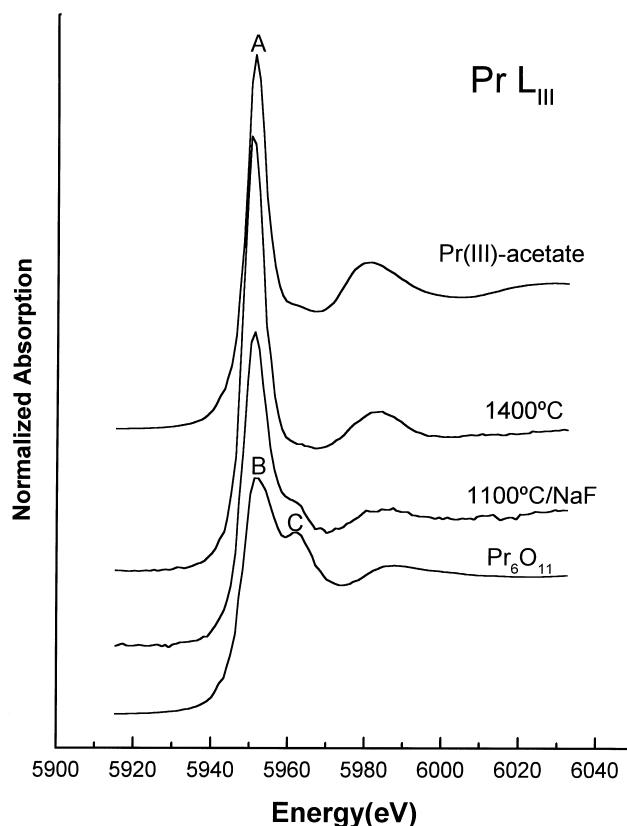


Fig. 7. Pr  $L_{\text{III}}$ -edge XANES spectra of the Pr-doped zircon sample heated at 1400°C in the absence of NaF and at 1100°C in the presence of NaF. The spectra of Pr (III) acetate and  $\text{Pr}_6\text{O}_{11}$  used as references are also included.

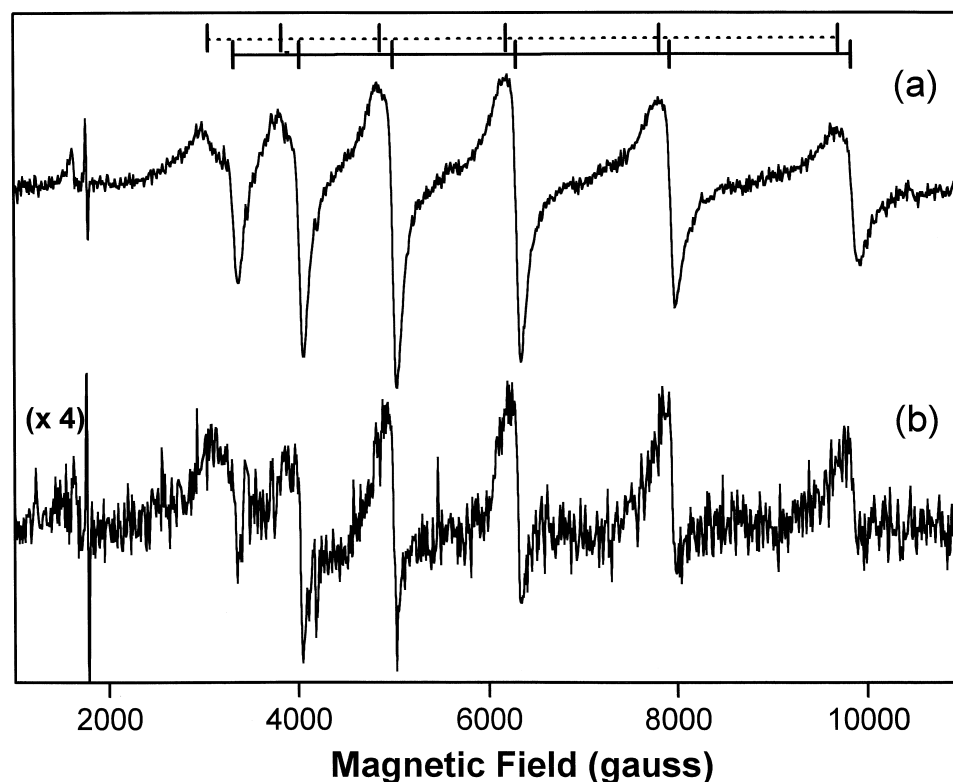


Fig. 6. EPR spectra measured at 10 K for the Pr-doped zircon samples: (a) heated at 1100°C in the presence of NaF and (b) heated at 1400°C in the absence of NaF. On the upper part of the plot, the parallel (continuous line) and perpendicular (dashed line) resonant positions calculated with the parameters given in Ref. 21 are also included.

5954 eV in the spectrum of the Pr-doped zircon powder heated in the presence of NaF, when compared to that of  $\text{Pr}_6\text{O}_{11}$ , suggests that this sample also contains a certain amount of  $\text{Pr}^{3+}$ . The latter could be related to a very small amount of the  $\text{Pr}_2\text{Zr}_2\text{O}_7$  phase associated to the very weak peak at  $d=3.09 \text{ \AA}$  detected by X-ray diffraction (Figs 4 and 5).

The unit cell parameters of zircon for the sample heated at  $1400^\circ\text{C}$  in the absence of NaF and at  $1100^\circ\text{C}$  in the presence of this flux were measured (Table 3) to gain information on the localisation of the Pr species in the zircon matrix. In the first case, the obtained parameters were found to be similar to those of undoped zircon, whereas in the presence of NaF, an increase of the unit cell volume was observed. These findings indicate the formation of a solid solution between Pr (IV) cations and the zircon lattice, which are only appreciably present in the sample when the firing is carried out in the presence of NaF. Such a solid solution must be then the main responsible of the strong yellow colour observed for the Pr doped zircon powders heated in the presence of fluxes, as it has been previously shown for commercial pigments.<sup>25</sup>

It should be noted that when the sample calcined at  $1100^\circ\text{C}$  in the presence of NaF was heated again at  $1400^\circ\text{C}$ , a significant decrease of the yellow colour intensity was observed as revealed by the important decrease of the  $b^*$  parameter from 54 at  $1100^\circ\text{C}$  to 35 at  $1400^\circ\text{C}$  (Table 2). This behaviour was accompanied by the almost complete disappearance of the Pr (IV) band (5965 eV) in the XANES spectrum of the sample (data not shown), which was similar to that of Pr (III) acetate (Fig. 7). This finding reveals an important decrease of the Pr (IV) content in the sample, which under these conditions show similar unit cell parameters to those of undoped zircon (Table 3). In addition, several weak peaks appeared in the X-ray diffraction pattern of the sample (Fig. 4), which can be attributed to  $\text{Pr}_8\text{Si}_6\text{O}_{24}$ .<sup>26</sup> These results strongly suggest that the Pr (IV)-zircon solid solution

**Table 3.** Unit cell parameters ( $a, c$ ) and unit cell volume ( $V$ ) measured for the Pr-doped zircon sample heated at different temperatures in the absence or the presence of NaF, and for a zircon blank. Parameters measured for a silicon standard added to the samples are also included. Errors are given in parentheses

Sample	a ( $\text{\AA}$ )	c ( $\text{\AA}$ )	V ( $\text{\AA}^3$ )
Zircon	6.6046(6) 5.4308(3) <sup>a</sup>	5.9798(5)	260.84(7)
1400°C	6.6045(3) 5.4311(3) <sup>a</sup>	5.9801(4)	260.85(4)
1100°C/NaF	6.612(1) 5.4313(6)	5.983(1)	261.6(1)
1100°C/NaF + 1400°C	6.6045(6)	5.9790(8)	260.80(8)

<sup>a</sup>Data referred to the silicon standard having an  $a$  parameter for 5.4309.

becomes unstable at  $1400^\circ\text{C}$ . Therefore, we can conclude that the main role of NaF in the preparation of yellow Pr-zircon pigments is to decrease the temperature of zircon formation to the range in which the chromophore responsible for the bright yellow colour, i.e. the Pr (IV)-zircon solid solution, is stable.

#### 4 Summary

The role that NaF plays in the preparation of Pr-doped zircon pigments was studied through the analysis of the nature and localisation of the Pr cations into the zircon matrix. The Pr-doped zircon powders were prepared by hydrolysis of liquid aerosols generated from metal alkoxides and  $\text{PrCl}_3$ . This procedure generates amorphous particles, which were calcined up to zircon formation in the absence and in the presence of NaF. In the first case, the complete formation of zircon took place after heating at  $1400^\circ\text{C}$ , at which temperature, a weak yellow colour resulted and the Pr cations mainly presented a threefold oxidation state being located out of the zircon lattice as  $\text{Pr}_2\text{Zr}_2\text{O}_7$ . In the presence of NaF, the minimum temperature required for zircon formation decreased to  $1100^\circ\text{C}$ . Under these conditions, most of the Pr cations showed a fourfold valence and formed a solid solution with the zircon lattice, which was responsible for the stronger yellow colour observed in this case. After heating this pigment at  $1400^\circ\text{C}$ , we detected an exsolution of the Pr (IV) cations as  $\text{Pr}_8\text{Si}_6\text{O}_{24}$  which was accompanied by a decrease of the yellow colour intensity. Therefore, it is concluded that the main role of NaF in the preparation of yellow Pr-zircon pigments is to decrease the temperature of zircon formation to the range in which the chromophore responsible for the bright yellow colour, i.e. the Pr (IV)-zircon solid solution, is stable.

#### Acknowledgement

This work was supported by the Spanish DGICYT under project PB95-0225.

#### References

1. Eppler, R. A., Zirconia based colors for ceramic pigments. *Ceram. Bull.*, 1977, **56**, 213–224.
2. Booth, F. T. and Peel, G. N., The preparation and properties of some zirconium stains. *Trans. J. Br. Ceram. Soc.*, 1962, **16**, 359–400.
3. Bell, B. T., The development of colorants for ceramics. *Rev. Prog. Coloration*, 1978, **9**, 48–56.
4. Oheim, R., Paulus, H. and Rüssel, C., Preparation of praseodymium-doped  $\text{ZrSiO}_4$  by a sol-gel route. *J. Mater. Sci. Letters*, 1991, **10**, 1171–1172.

5. Shoyama, M., Nasu, H. and Kamiya, K., Preparation of rare-earth-zircon pigments by the sol-gel method. *J. Ceram. Soc. Japan*, 1998, **106**, 279–284.
6. Eppler, R. A., Formation of praseodymium-doped zircon colors in the presence of halides. *Ind. Eng. Chem. Prod. Res. Develop.*, 1971, **10**, 352–355.
7. Wildblood, N. C., Fluorine in ceramic colours. *Trans. J. Brit. Ceram. Soc.*, 1973, **72**, 31–33.
8. Trojan, M., Synthesis of a yellow zircon pigment. *Dyes and Pigments*, 1988, **9**, 261–273.
9. Tartaj, P., Serna, C. J. and Ocaña, M., Preparation of blue vanadium-zircon pigments by aerosols hydrolysis. *J. Am. Ceram. Soc.*, 1995, **78**, 1147–1152.
10. Tartaj, P., Soria, J., Serna, C. J. and Ocaña, M., Vanadium-doped zirconia: preparation by hydrolysis of aerosols and origin of pigment colour. *J. Mater. Res.*, 1998, **13**, 413–420.
11. Ocaña, M. and Martínez-Gallego, M., Preparation by hydrolysis of aerosols and properties of Cr, Mn and Co doped alumina spherical particles. *Colloid & Polymer Sci.*, 1997, **275**, 1010–1107.
12. Ocaña, M., González-Elípe, A. R., Andrés-Vergés, M., Tartaj, P., Serna, C. J. and Orera, V. M., Preparation by hydrolysis of aerosols and colour properties of Cr-doped and Co-doped zircon powders. *J. European Ceram. Soc.*, 1998, **18**, 821–830.
13. Tartaj, P., Sanz, J., Serna, C. J. and Ocaña, M., Zircon formation from amorphous spherical  $ZrSiO_4$  particles obtained by hydrolysis of aerosols. *J. Mater. Sci.*, 1994, **29**, 6533–6538.
14. Tartaj, P., González-Carreño, T., Serna, C. J. and Ocaña, M., Iron zircon pigments prepared by pyrolysis of aerosols. *J. Solid State Chem.*, 1997, **128**, 102–108.
15. ASTM card no. 6 266.
16. Natl. Bur. Stand. (U.S.) Monogr. 25;1335;1976.
17. Bonin, D., Kaiser, P., Fretigny C. and Desbarres, J., In *Structures Fines d'Absorption des Rayons X en Chimie*, Vol. 3, ed. H. Dexpert, A. Michalowicz and M. Verdager. Orsay, 1989.
18. C.I.E., Recommendations on uniform colour spaces, colour difference equations, psychometrics colour terms. Supplement no. 2 of C.I.E. publ. no. 15 (E1-1.31) 1971. Bureau Central de la C.I.E., Paris, 1978.
19. Lefèvre, J., Contribution a l'étude de différentes modifications structurales des phases de type fluorine dans les systèmes a base de zircone ou d'oxyde de hafnium. *Ann. Chim.*, 1963, **8**, 117–149.
20. ASTM card no. 17-923.
21. Tartaj, P., Moya, J. S., Requena, J., de Aza, S., Guitián, F., Serna, C. J. and Ocaña, M., The formation of zircon from amorphous  $ZrO_2(SiO_2)$  powders. *J. Mater. Sci.*, 1996, **31**, 6089–6094.
22. ASTM card no. 19-1021.
23. Harris, E. A., Mellor, J. H. and Parke, S., Electron paramagnetic resonance of tetravalent praseodymium in zircon. *Phys. Stat. Sol (b)*, 1984, **122**, 757–760.
24. Bianconi, A., Marcelli, A., Dexpert, H., Karnatak, R., Kotani, A., Jo, T. and Petiau, J., *Phys. Rev. B*, 1987, **35**, 806.
25. Ocaña, M., Caballero, A., González-Elípe, A. R., Tartaj, P. and Serna, C. J., Valence and localization in Pr-doped zircon. *J. Solid State Chem.*, 1998, **139**, 412–415.
26. ASTM card No. 23-1389.